Journal of Electronic Materials
https://doi.org/10.1007/s11664-026-12729-w

TOPICAL COLLECTION: 67TH ELECTRONIC MATERIALS CONFERENCE 2025

Quaternary i-MAX Phases $(Mo_{2/3}RE_{1/3})_2AlC$ (RE: Dy, Tb, Er): Experimental Characterization and First-Principles Insights into their Fundamental Properties

Nisha H. Makani[1] · Chandra M. Adhikari[1] · Binod K. Rai[2] · Bhoj Gautam[1]

Received: 16 October 2025 / Accepted: 4 February 2026

Abstract
Rare earth (RE)-based materials have unique electronic, magnetic, and optical properties, leading to the recent discovery of atomically layered solids with the chemical formula $(M'_{2/3}RE_{1/3})_2AlC$, which have since garnered significant attention in the scientific community. This study aims to synthesize, characterize, and investigate the structural and thermal stability of the RE i-MAX phases. We prepared i-MAX phases using molybdenum (Mo) as M′ and RE elements as Dy, Tb, and Er, namely $(Mo_{2/3}Dy_{1/3})_2AlC$, $(Mo_{2/3}Tb_{1/3})_2AlC$, and $(Mo_{2/3}Er_{1/3})_2AlC$. Structural characterization through x-ray diffraction (XRD) and Raman spectroscopy confirms the formation of the RE-based i-MAX phase, along with the presence of minor impurity phases in the alloys. Thermogravimetric analysis (TGA) conducted up to 1000°C under ambient conditions reveals that the i-MAX phases remain thermally stable up to approximately 450°C, beyond which oxidation leads to a noticeable weight gain in all samples. Differential scanning calorimetry (DSC) measurements during heating and cooling cycles show endothermic and exothermic peaks for $(Mo_{2/3}Dy_{1/3})_2AlC$ i-MAX in the 410–420°C range, indicating a temperature-induced minor atomic arrangement. In contrast, these peaks are absent in the Tb- and Er-based i-MAX phases. These findings offer valuable insights into the thermal behavior and stability of these i-MAX phases under thermal stress, contributing to a deeper understanding of their unique properties. Furthermore, first-principles density functional theory (DFT) calculations were performed to investigate the electronic and optical properties of the i-MAX phases. The results reveal their metallic nature, with pronounced contributions from Mo and RE elements near the Fermi level and within the conduction band.

Keywords Rare earth · i-MAX · thermal stability · structural · electronic · optical

Introduction

Rare earth elements (REEs), including the lanthanides (La, Ce, Pr, Nd, Pm, Sm, Eu, Gd, Tb, Dy, Ho, Er, Tm, Yb, and Lu), along with Sc and Y, are essential for modern technologies. Over the past three decades, their applications have expanded to include computer memory, rechargeable batteries, super magnets, solar panels, and superconductors.[1] REEs have recently been employed in the synthesis of MAX phase systems, well-known for their excellent properties, and have gained significant attention after the discovery of MXenes.[2] Initially, MAX phases were developed as ternary compounds with the formula M_2AX (M = Ti, Zr, Hf, V, Nb, Ta, Cr, Mo; A = Al, Si, etc.; X = C and/or N) and later expanded to the general structure $M_{n+1}AX_n$ (n = 1–4).[2,3] Beyond these $M_{n+1}AX_n$ phases, incorporating different M, A, and X elements, with more than three elements mixing in each sites, e.g. $(Ti_{1-x}Cr_x)_2AlC$ (M-site mixing),[4] $Cr_2(Al_{1-x}Ge_x)C$ (A-site mixing),[5] $Ti_2Al(C_{1-x}N_x)_y$ (X site mixing),[6] $(Ti_{0.33}Zr_{0.16}V_{0.61}Nb_{0.16}Ta_{0.16})_2Al(C_xN_{1-x})$ (multi-site mixing), leads to the formation of complex MAX phases with novel properties. However, mixing these elements in specific ratios results in the formation of chemically ordered MAX phases. This ordering can occur either along the out-of-plane or in-plane direction. The ordered MAX phase with chemical formula $M'_2\,M''_nAX_{n+1}$ where M′ and M″ occupy an atomic layer, respectively, with M′

✉ Bhoj Gautam
bgautam@uncfsu.edu

[1] Department of Chemistry, Physics and Materials Science, Fayetteville State University, Fayetteville, North Carolina 28301, USA

[2] Savannah River National Laboratory, Aiken, South Carolina 29808, USA

Published online: 23 February 2026

encapsulated by an A-atomic layer in the outer layer and M″ encapsulated by an X-atomic layer in the inner layer are named as o-MAX phase.[7] In this phase, the ordering of metal atoms is along the stacking direction of the layers. Whereas, some ordered MAX phases with chemical formula $(M'_{2/3}\,M''_{1/3})_2AX$ where M′ and M″ are chemically ordered within the basal planes, are referred to as i-MAX phase. In this phase, M′ forms a honeycomb lattice, with M″ positioned at the center of each hexagon.[2,8,9] The first ordered o-MAX phase, Cr_2TiAlC_2, was discovered in 2014 by heating a 1:1 ratio of Cr_2AlC and TiC at a specific temperature in an Argon atmosphere.[2,10] In 2017, Tao et al. synthesized the first quaternary in-plane MAX phase $(Mo_{2/3}Sc_{1/3})_2AlC$.[11] This material exhibited in-plane ordering of Mo and Sc, a distinctive feature compared with traditional MAX phases. This new i-MAX phase was subsequently used to produce MXenes, sparking further research into i-MAX phases incorporating REEs, such as $(Mo_{2/3}RE_{1/3})_2AlC$, $(Mo_{2/3}Y_{1/3})_2AlC$, $(W_{2/3}Y_{1/3})_2AlC$, $(Mo_{2/3}RE_{1/3})_2AlC$, $(W_{2/3}RE_{1/3})_2AlC$, and $(Mo_{2/3}RE_{1/3})_2GaC$.[12–18] These novel i-MAX phases are prepared using usually pressureless sintering, and, according to reported literature, RE i-MAX phases exhibit additional impurity phases in addition to the main i-MAX phases.[16,19] Since then, extensive theoretical and experimental studies have investigated the electronic structure, magnetism, and mechanical properties of newly discovered i-MAX phases, which exhibit characteristics closely resembling those of conventional MAX phases.[9,15]

MAX phases are promising materials, particularly for applications such as protective coating in fuel cladding for nuclear reactors.[20,21] In addition, their use in aerospace applications requires an investigation of oxidation resistance at elevated temperatures.[22] At high temperatures, oxidation can alter mechanical properties; therefore, research into oxidation and thermal stability is essential.[23–25] During oxidation, MAX phases form a stable, protective oxide layer; in particular, Al-, Si-, and Cr-based MAX phases generate Al_2O_3, SiO_2, and Cr_2O_3 coatings, respectively, at high temperatures.[26] These oxide layers are a result of higher diffusivity and chemical activity of A elements compared to M elements, which makes the MAX phase prone to oxidation in an oxidizing environment.[26] Early investigations of oxidation behavior focused on Ti_3SiC_2, Ti_2AlC, Cr_2AlC, and Ti_3AlC_2, followed by studies on recently developed MAX and i-MAX phases.[27,28] A comparative study of high temperature oxidation of Cr_2AlC MAX phase and $(Cr_{2/3}Lu_{1/3})_2AlC$ i-MAX phase has been carried out by Sun et al.[29] with different oxidation products, such as the formation of garnet-type phase ($Lu_3(Cr,Al)_5O_{12}$), indicating characteristic effects of RE i-MAX phase, showing RE-O affinity is more stable than RE-C.[29] These i-MAX phase materials are characterized by unique properties including electrical and thermal conductivities, light weight, robust to high temperature, and have shown great potential in spintronics, thermoelectric, magnetic sensors, catalysis, etc.[30,31] Therefore, the structural and thermal characterization of RE-based i-MAX phase materials will provide significant interest to both theoreticians and experimentalists working in these areas. In this study, the structural properties of the quaternary i-MAX phases $(Mo_{2/3}Dy_{1/3})_2AlC$, $(Mo_{2/3}Tb_{1/3})_2AlC$, and $(Mo_{2/3}Er_{1/3})_2AlC$ were examined using XRD and Raman spectroscopy, while their thermal stability was evaluated through TGA and DSC measurements. Furthermore, the fundamental electronic and optical properties of all three i-MAX phases were examined using first-principles DFT calculations. Our study provides valuable insights into thermal, structural, and optoelectronic properties of RE-based i-MAX phase materials.

Materials and Methods

Synthesis of $(Mo_{2/3}RE_{1/3})_2AlC$ i-MAX Phase

To synthesize the RE i-MAX phase $(Mo_{2/3}RE_{1/3})_2AlC$, (RE: Dy, Tb, Er) specific ratios of all required materials were used, including Mo (Thermo Fisher Scientific, powder, 99.95), C (Sigma Aldrich, powder, 99.99%), Dy, Tb, and Er (Ames Laboratory), and Al (Alfa Aesar, 99.999%). The synthesis was carried out using arc melting, set up under an inert argon atmosphere. Initially, Mo and C powders were mixed in the desired atomic ratio using a mortar and pestle to obtain a homogeneous blend, which was then mechanically pressed into pellets. Subsequently, Al and RE (Dy, Tb, Er) were added in the appropriate weight ratios, and the mixture was arc-melted using an Edmund Bühler electric arc furnace. The mixture was then melted in an electric arc furnace.[30,32] To achieve a homogeneous alloy, the prepared sample was remelted 4–5 times. The sample is then annealed for 10 days at 800°C in a sealed quartz tube under argon.

Experimental Section

Structural phases of the prepared samples were confirmed using x-ray diffraction (Rigaku Miniflex) with Cu K_α radiation wavelength 1.5406 Å, and Raman spectroscopy (Horiba) with laser 532 nm with 10% laser power with a range from 60 cm^{-1} to 1200 cm^{-1}. Thermal attributes were studied using a Thermogravimetric Analyser (TGA) (Shimadzu) in ambient conditions from room temperature to 1000°C under ambient conditions and a differential scanning calorimetry (DSC) (Shimadzu) from room temperature to 500°C in a nitrogen environment.

Computational Method

A theoretical study was conducted using first-principles density functional theory (DFT) calculations implemented in the Vienna ab initio simulation package (VASP).[33,34] Experimentally observed C2/c symmetric crystal structures were taken as initial structures and fully relaxed, minimizing energy and force with convergence criteria of 10^{-6} eV and 10^{-2} eV/Å, respectively. Projector augmented wave method-based pseudopotentials and Perdew–Burke–Ernzerhof functionals were used to address ion–electron interactions and exchange correlations, respectively.[35–37] The plane wave cut-off energy of 520 eV was used. The Γ-centered automatic *k*-point meshes of 12 × 12 × 3 were chosen for Brillouin zone sampling for all i-MAX phases in such a way that *k*-point spacing is approximately 0.2/Å in each direction in reciprocal space. We used supercells of 2 × 2 × 3 to carry out theoretical investigation of all i-MAX phases.

Results and Discussion

Structural Properties

Figure 1a illustrates the chemical structure representation of the RE i-MAX phase along [100] zone axis, where RE and the Mo atoms display an in-plane ordering, and RE atoms are located out of the Mo planes. This protruding arrangement highlights the characteristic in-plane ordered RE occupation within the Mo-C layers. Figure 1b shows

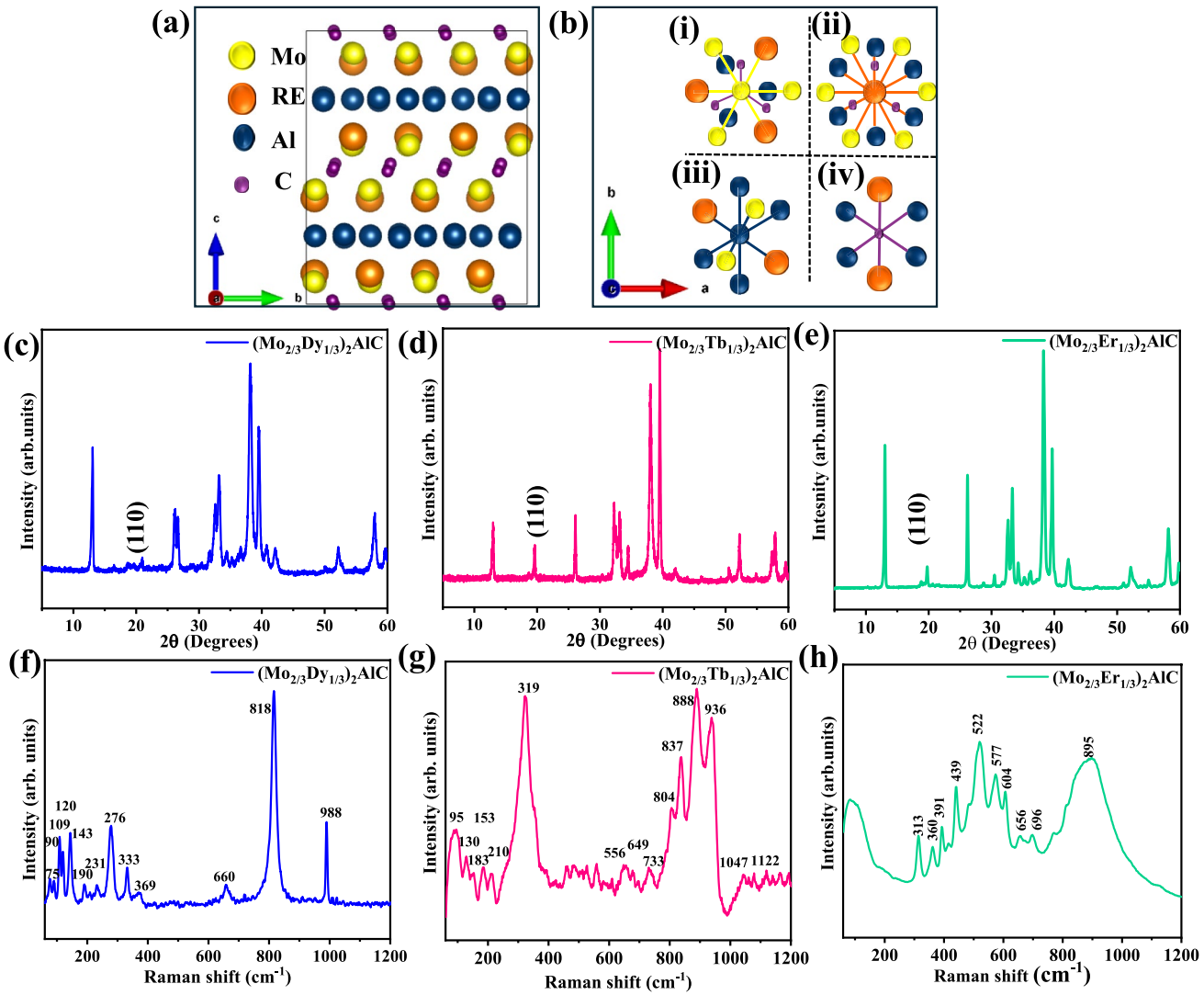

Fig. 1 (a) Illustration of crystal structure the RE i-MAX phase structure, (b) atomic surrounding is schematically illustrated for (i) Mo, (ii) RE, (iii) Al, and (iv) C seen from top view, (c, d, e) x-ray diffraction (XRD) (f, g, h) Raman spectra of $(Mo_{2/3}Dy_{1/3})_2AlC$, $(Mo_{2/3}Tb_{1/3})_2AlC$ and $(Mo_{2/3}Er_{1/3})_2AlC$ i-MAX samples, respectively

local atomic coordination for the RE i-MAX. Mo atoms have three C as nearest neighbor (NN), three Al as next NN (NNN), three Mo as third NN (TNN), and RE as fourth NN (Fig. 1b(i)). RE atoms have three C as NN, six Mo as NNN, and six Al as TNN (Fig. 1b(ii)). Figure 1b(iii) shows each Al atom has four Al as NN, two Mo as NNN, and two RE as TNN. The carbon atoms have four Mo as NN and two RE as TNN (Fig. 1b(iv)). The XRD pattern of the polycrystalline $(Mo_{2/3}Dy_{1/3})_2AlC$, $(Mo_{2/3}Tb_{1/3})_2AlC$ and $(Mo_{2/3}Er_{1/3})_2AlC$ powder is shown in Fig.1c, d, e respectively. XRD peaks match the reported data, which indicates that RE i-MAX phases have been successfully prepared with a phase C2/c monoclinic structure.[38] In i-MAX phases, the primary XRD feature is a peak around 20°, which corresponds to the interplanar spacing originates purely due to the Mo/RE in-plane chemical ordering.[39] This peak is absent in ternary MAX phases. In the case of Dy, Tb, and Er i-MAX phases, the (110) peaks at 20°, 19.65°, and 19.74°, corresponding to interplanar distances of 0.48 nm, 0.45 nm, and 0.48 nm, respectively. The vibrational properties of the synthesized i-MAX phases were analyzed, and the corresponding Raman shifts are illustrated in Fig. 1f-h. To date, no theoretical or experimental Raman investigations have been reported on Tb-based i-MAX phases. However, studies on the phonon vibrational characteristics of Dy- and Er-based i-MAX phases are available in the literature, following the Raman analysis framework established by Champagne et al.[40] The low-frequency modes primarily arise from the collective vibrations of RE, Mo, and Al atoms. The mid-frequency region is dominated by the coupled vibrations of Mo and Al atoms, while the high-frequency modes are mainly attributed to the characteristic vibrations of carbon atoms within the structure. The Raman shifts observed at (70–200) cm^{-1} are attributed to the vibrational modes of RE, Mo, and Al.[40] Raman shifts at (200–270) cm^{-1} originate from vibrational modes of Al and Mo.[40] High frequency modes correspond to vibration peaks at 333 cm^{-1} and 369 cm^{-1} in Dy-based i-MAX phase are associated with Dy_2O_3.[41] The prominent Raman bands observed in the range of 750–990 cm^{-1} for all three samples can be attributed to the vibrational modes of Mo-O bonds.[42] These findings suggest the presence of oxide impurities or partial surface oxidation in the RE-based i-MAX phase, likely induced by localized heating from the laser during Raman measurements.[14,43]

The thermal properties of the RE i-MAX phase were investigated using TGA and DSC measurements. Figure 2a, b, and c present the TGA and DTA profiles under ambient environment for the Dy, Tb, and Er-based i-MAX phases, respectively, recorded from room temperature to 1000°C. All three i-MAX phases remain stable up to ~450°C, beyond which oxidation occurs, leading to oxide formation and the appearance of exothermic peaks at ~710°C for Dy, ~704°C for Tb, and ~761°C for Er-based i-MAX phases. These processes correspond to weight gains of approximately 20%, 30%, and 25% for the Dy, Tb, and Er samples, respectively. At higher temperatures, weight reduction begins around 832°C (Dy), 838°C (Tb), and 834°C (Er). As the measurements were carried out up to 1000°C, only the onset of this weight loss was observed. Figure 2d, e, and f display the DSC profiles. In

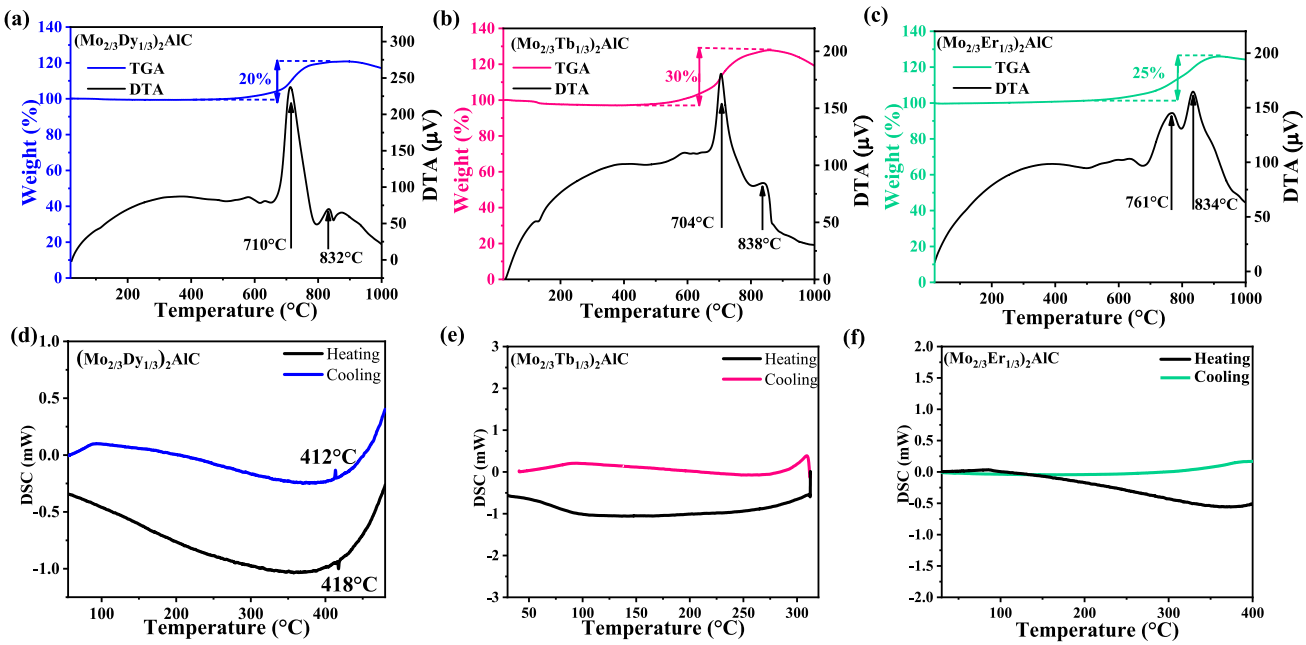

Fig. 2 (a, b, c) TGA and DTA (d, e, f) DSC profiles of $(Mo_{2/3}Dy_{1/3})_2AlC$, $(Mo_{2/3}Tb_{1/3})_2AlC$, and $(Mo_{2/3}Er_{1/3})_2AlC$ i-MAX phase, respectively

the Dy-based i-MAX phase, endothermic and exothermic peaks are observed near to 415°C, where these peaks are absent in the Tb and Er-based i-MAX phases. *In situ* temperature-dependent XRD measurements (Supplementary Fig. S1a) were carried out on $(Mo_{2/3}Dy_{1/3})_2AlC$ i-MAX phase to verify any structural phase transitions. The XRD patterns recorded at room temperature and 450°C display nearly identical features, suggesting that the structure remains stable without any phase transformation at higher temperatures. A detailed examination of the XRD pattern within the 35°–40° range (Supplementary Fig. S1b) reveals a slight shift of the diffraction peaks toward lower angles at 450°C relative to room temperature in the Dy-based i-MAX phase, indicating a minor expansion in the interplanar spacing.

Figure 3a, b, c presents the band structures of all three RE-based i-MAX phases, illustrating the variation of energy (E) relative to the Fermi level (E_F) along the high-symmetry paths. The corresponding projected density of states (PDOS), Fig. 3d, e, f, depicts the distribution of available electronic states per atom within each energy range (per eV) as a function of E-E_F. The minute details of band structures and density of states are not the same; however, all three i-MAX phases are metallic. In addition, Mo-4d, RE−5d, and C-2p contribute the most to the PDOS at and around the Fermi level.

Dielectric function (ε) is the fundamental quantity in understanding the optical properties of materials that characterize material response to electric fields, bridging quantum electronic structure and microscopic optical response. It is an energy-dependent complex quantity whose real part describes dispersion, the polarizability of materials, and their energy storage capacity. In contrast, the imaginary part relates to energy absorption, dissipation, and interband transitions. Dielectric functions as a function of energy for all three i-MAX phases studied here are presented in Fig. 4. Insets in Fig. 4 show the dielectric functions in the energy ranges of the visible spectrum. The imaginary parts of dielectric functions are mostly positive, as one expects for passive lossy materials. We observed significantly high positive values for the real parts of ε, indicating in-plane polarization with dielectric-like behavior from zero energy to the mid-infrared (IR) region. In the near-IR range, we observe negative Re ε showing metal-like behavior with in-plane polarization of the i-MAX phases with an external field. At the visible spectrum and beyond, both the real and imaginary values asymptotically approach their static values.

Optical conductivities describe how materials conduct current under an oscillating field and absorb photon energy from the field. Component-resolved optical conductivities of all three i-MAX phases are presented in Fig. 5. The slab thickness of 100 Å and inverse Drude lifetime of

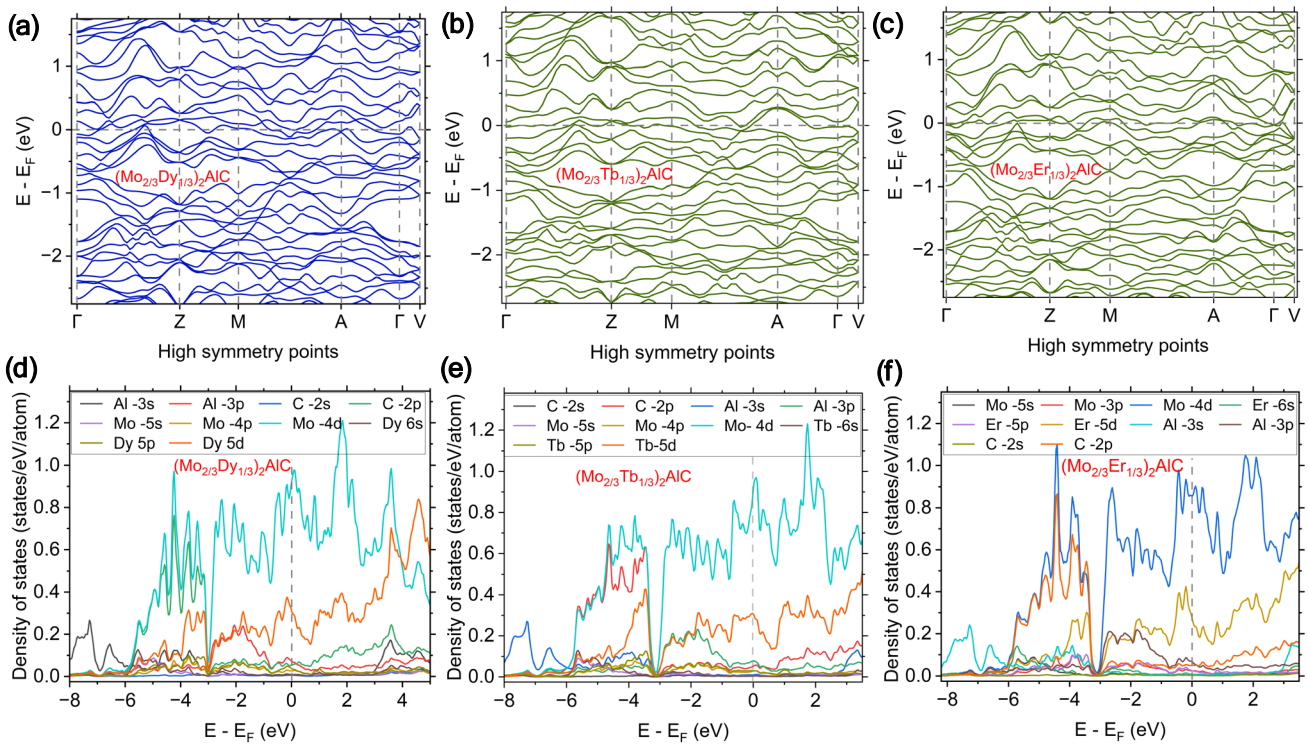

Fig. 3 Band structure (a, b, c) and orbital resolved density of states (d, e, f) of $(Mo_{2/3}Dy_{1/3})_2AlC$, $(Mo_{2/3}Tb_{1/3})_2AlC$, and $(Mo_{2/3}Er_{1/3})_2AlC$ i-MAX phases, respectively

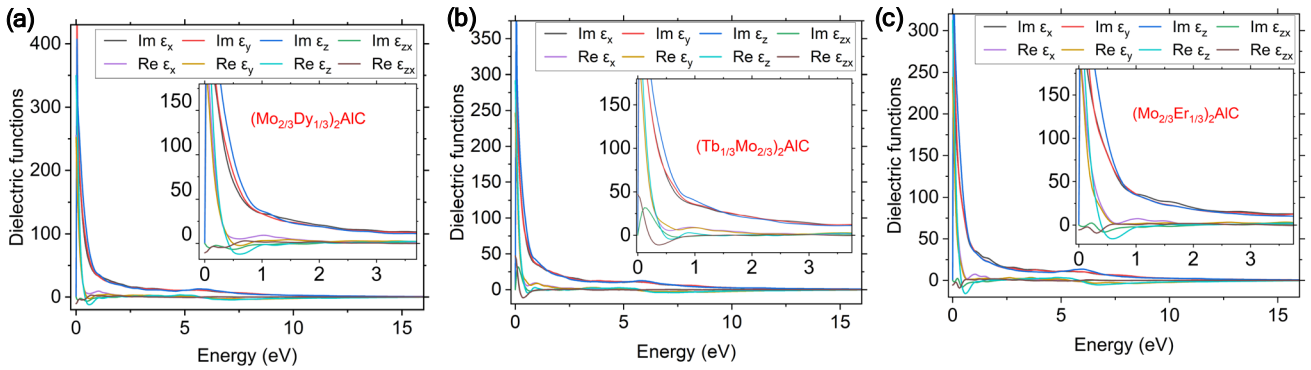

Fig. 4 Dielectric functions of (a) $(Mo_{2/3}Dy_{1/3})_2AlC$, (b) $(Mo_{2/3}Tb_{1/3})_2AlC$, (c) and $(Mo_{2/3}Er_{1/3})_2AlC$ i-MAX phases

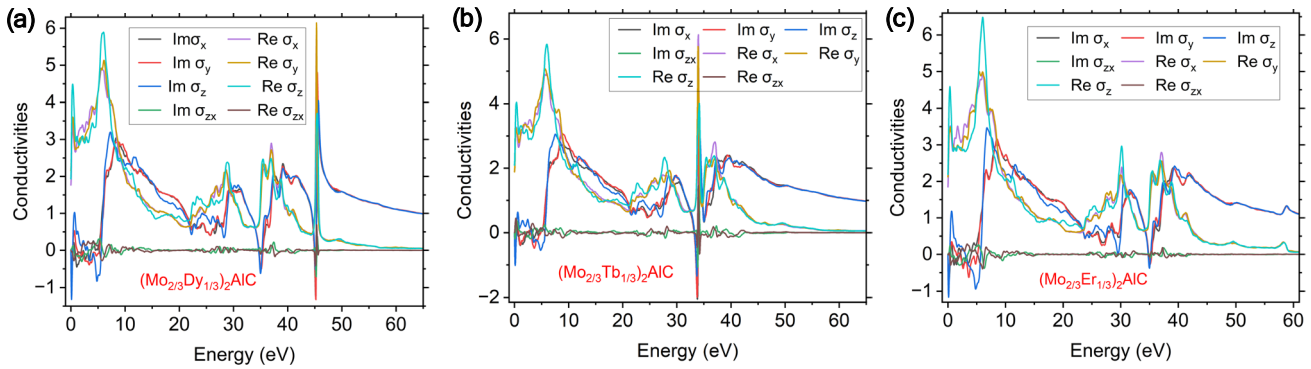

Fig. 5 Conductivities of (a) $(Mo_{2/3}Dy_{1/3})_2AlC$, (b) $(Mo_{2/3}Tb_{1/3})_2AlC$, and (c) $(Mo_{2/3}Er_{1/3})_2AlC$ i-MAX phases

$1/\tau \sim 4.56 \times 10^{14} s^{-1}$ was used, which in the energy scale is about 0.3 eV. The variation of optical conductivities with energy indicates the tunable dielectric modulation in i-MAX phases. The conductivities variation with energy looks similar at energy range from zero energy to far ultraviolet (UV) ~10 eV, while energies where conductivities have resonance peaks at extreme far UV differ from one i-MAX to another.

Conclusions

In this study, RE-based i-MAX phases were successfully synthesized using the arc melting method. XRD analysis confirmed the formation of the Dy, Tb, Er-based in-plane ordered i-MAX structure, characterized by the peak at ~20° correspond to ordered arrangement of Mo and RE atoms. Raman spectroscopy further revealed the characteristic vibrational modes corresponding to RE, Mo, and Al atoms, along with additional oxide-related peaks, which likely originate either from inherent oxide impurities formed during synthesis or from localized laser-induced heating during Raman measurements. All the i-MAX phases exhibited thermal stability up to 450°C, beyond this temperature, gradual oxidation was observed in air owing to the high oxidation affinity of RE and Mo elements. Moreover, DSC measurements confirmed the absence of any structural or phase transitions within this temperature range, supporting the thermal robustness of the in-plane ordered i-MAX phases. Density functional theory calculations show all three i-MAX phases are metallic. The electronic density of states in i-MAX phases is mainly dominated by the 4d orbitals of Mo and 2p orbitals of C, with substantial contributions from the 5d states of REE near and around the Fermi level.

Supplementary Information The online version contains supplementary material available at https://doi.org/10.1007/s11664-026-12729-w.

Acknowledgments This work was supported by the U.S. Department of Energy (DOE), Office of Science, Office of Basic Energy Sciences, under award number DESC0024611. SRNL work was produced by Battelle Savannah River Alliance, LLC under Contract No. 89303321CEM000080 with the U.S. Department of Energy. Publisher acknowledges the U.S. Government license to provide public access

under the DOE Public Access Plan (http://energy.gov/downloads/doe public-access-plan).

Funding Open access funding provided by the Carolinas Consortium. Basic Energy Sciences, DE-SC0024611, Bhoj Raj Gautam

Conflict of Interest The authors have no known conflicts of interest to declare.

References

1. V. Balaram, A review of applications, occurrence, exploration, analysis, recycling, and environmental impact. *Geosci. Front.* 10, 1285 (2019).
2. M. Dahlqvist, M.W. Barsoum, and J. Rosen, MAX phases—Past, present, and future. *Mater. Today* 72, 1 (2024).
3. M.S. Alam, M.A. Chowdhury, M.A. Kowser, M.S. Islam, M.M. Islam, and T. Khandaker, Advances of MAX phases: synthesis, characterizations, and challenges. *Eng. Rep.* 6, e12911 (2024).
4. J.C. Schuster, H. Nowotny, and C. Vaccaro, The ternary systems: CrAlC, VAlC, and TiAlC and the behavior of H-phases (M_2AlC). *J. Solid State Chem.* 32, 213 (1980).
5. T. Cabioch, P. Eklund, V. Mauchamp, M. Jaouen, and M.W. Barsoum, Tailoring of the thermal expansion of $Cr_2(Al_x,G_{e1-}x)C$ phases. *J. Eur. Ceram. Soc.* 33, 897 (2013).
6. T. Cabioc'h, P. Eklund, V. Mauchamp, and M. Jaouen, Structural investigation of substoichiometry and solid solution effects in Ti2Al(Cx, N1–x)y compounds. *J. Eur. Ceram. Soc.* 32, 1803 (2012).
7. B. Wen, Y. Liu, L. Cao, X. San, Y. Zhou, M. Jiang, L. Chu, Q. Feng, and C. Hu, Synthesis of two new o-MAX phases Mo_2VAlC_2 and $Mo_2V_2AlC_3$ and their derivatives o-MXene $Mo_2VC_2T_x$ and $Mo_2V_2C_3T_x$. *J. Eur. Ceram. Soc.* 45, 116964 (2025).
8. N.H. Makani, B.K. Rai, B.P. Bastakoti, A. Bretana, and B. Gautam, Current advances in i-MAX phases and their two dimensional derivative i-MXenes: challenges and opportunities. *Adv. Electron. Mater.* 11(21), e00478 (2025).
9. M. Khazaei, V. Wang, C. Sevik, A. Ranjbar, M. Arai, and S. Yunoki, Electronic structures of iMAX phases and their two-dimensional derivatives: a family of piezoelectric materials. *Phys. Rev. Mater.* 2, 074002 (2018).
10. Z. Liu, E. Wu, J. Wang, Y. Qian, H. Xiang, X. Li, Q. Jin, G. Sun, X. Chen, J. Wang, and M. Li, Crystal structure and formation mechanism of $(Cr_{2/3}Ti_{1/3})_3AlC_2$ MAX phase. *Acta Mater.* 73, 186 (2014).
11. Q. Tao, M. Dahlqvist, J. Lu, S. Kota, R. Meshkian, J. Halim, J. Palisaitis, L. Hultman, M.W. Barsoum, P.O. Persson, and J. Rosen, Two-dimensional $Mo_{1.33}C$ MXene with divacancy ordering prepared from parent 3D laminate with in-plane chemical ordering. *Nat. Commun.* 8(1), 14949 (2017).
12. M. Dahlqvist, A. Petruhins, J. Lu, L. Hultman, and J. Rosen, Origin of chemically ordered atomic laminates (i-MAX): expanding the elemental space by a theoretical/experimental approach. *ACS Nano* 12, 7761 (2018).
13. X. Feng, T. Bai, and B. Xiao, Prediction of surface termination preference of out-of-plane ordered double-transition metal MXenes (o-MXenes) from first-principles calculations. *J. Phys. Conf. Ser.* 2321, 012012 (2022).
14. A. Petruhins, J. Lu, L. Hultman, and J. Rosen, Synthesis of atomically layered and chemically ordered rare-earth (RE) i-MAX phases; $(Mo_{2/3}RE_{1/3})_2GaC$ with RE = Gd, Tb, Dy, Ho, Er, Tm, Yb, and Lu. *Mater. Res. Lett.* 7, 446 (2019).
15. A. Champagne, F. Ricci, M. Barbier, T. Ouisse, D. Magnin, S. Ryelandt, T. Pardoen, G. Hautier, M.W. Barsoum, and J.C. Charlier, Insights into the elastic properties of RE- i -MAX phases and their potential exfoliation into two-dimensional RE- i -MXenes. *Phys. Rev. Mater.* 4, 013604 (2020).
16. Q. Tao, M. Barbier, A. Mockute, C. Ritter, R. Salikhov, U. Wiedwald, S. Calder, C. Opagiste, R.M. Galera, M. Farle, T. Ouisse, and J. Rosen, Magnetic phase diagram of $(Mo_{2/3}RE_{1/3})_2AlC$, RE = Tb and Dy, studied by magnetization, specific heat, and neutron diffraction analysis. *J. Phy. Condens. Matter* 34, 215801 (2022).
17. J. Yang, R. Liu, N. Jia, K. Wu, X. Fu, Q. Wang, and W. Cui, Novel W-based in-plane chemically ordered $(W_{2/3}R_{1/3})_2AlC$ (R = Gd, Tb, Dy, Ho, Er, Tm and Lu) MAX phases and their 2D $W_{1.33}C$ MXene derivatives. *Carbon* 183, 76–83 (2021).
18. R. Meshkian, M. Dahlqvist, J. Lu, B. Wickman, J. Halim, J. Thörnberg, Q. Tao, S. Li, S. Intikhab, J. Snyder, M.W. Barsoum, M. Yildizhan, J. Palisaitis, L. Hultman, P.O.Å. Persson, and J. Rosen, W-Based atomic laminates and their 2D derivative $W_{1.33}C$ MXene with vacancy ordering. *Adv. Mater.* 30, 1706409 (2018).
19. J. Yang, G. Yao, S. Sun, Z. Chen, S. Yuan, K. Wu, X. Fu, Q. Wang, and W. Cui, Structural, magnetic properties of in-plane chemically ordered $(Mo_{2/3}R_{1/3})_2AlC$ (R = Gd, Tb, Dy, Ho, Er and Y) MAX phase and enhanced capacitance of $Mo_{1.33}C$ MXene derivatives. *Carbon* 179, 104 (2021).
20. D. Horlait, S. Grasso, A. Chroneos, and W.E. Lee, Attempts to synthesise quaternary MAX phases $(Zr,M)_2AlC$ and $Zr_2(Al,A)C$ as a way to approach Zr_2AlC. *Mater. Res. Lett.* 4, 137 (2016).
21. L.F. He, Y.W. Bao, M.S. Li, J.Y. Wang, and Y.C. Zhou, Oxidation of $Zr_2[Al(Si)]_4C_5$ and $Zr_3[Al(Si)]_4C_6$ in air. *J. Mater. Res.* 23, 3339 (2008).
22. N. Prasad, and R. Wanhill eds., *Aerospace Materials and Material Technologies*. (Singapore: Springer, 2017)., p.455.
23. S.N. Perevislov, T.V. Sokolova, and V.L. Stolyarova, The Ti_3SiC_2 max phases as promising materials for high temperature applications: formation under various synthesis conditions. *Mater. Chem. Phys.* 267, 124625 (2021).
24. M. Guo, G. Cao, H. Pan, J. Guo, C. Chen, B. Zhang, and J. Hu, Recent progress in synthesis of MAX phases and oxidation & corrosion mechanism: a review. *Mater. Res. Lett.* 12, 765 (2024).
25. D.J. Tallman, B. Anasori, and M.W. Barsoum, A critical review of the oxidation of Ti_2AlC, Ti_3AlC_2 and Cr_2AlC in Air. *Mater. Res. Lett.* 1, 115 (2013).
26. D. Sauceda, P. Singh, A.R. Falkowski, Y. Chen, T. Doung, G. Vazquez, M. Radovic, and R. Arroyave, High-throughput reaction engineering to assess the oxidation stability of MAX phases. *Npj Comput. Mater.* 7, 1 (2021).
27. M.W. Barsoum, L.H. Ho-Duc, M. Radovic, and T. El-Raghy, Long time oxidation study of Ti_3SiC_2, Ti_3SiC_2 / SiC, and Ti_3SiC_2 / TiC composites in air. *J. Electrochem. Soc.* 150, B166 (2003).
28. J. Wang, and Y. Zhou, Long time oxidation study of Ti_3SiC_2, Ti_3SiC_2 / SiC, and Ti_3SiC_2 / TiC composites in air. *Annu. Rev. Mater. Res.* 39, 415 (2009).

29. S. Sun, Z. Ma, Z. Chen, P. Liu, Y. Song, Q. Lu, X. Fu, Q. Wang, and W. Cui, The crystallographic structure and properties of novel quaternary nanolaminated rare-earth-Cr-based i-MAX phases. *Acta Mater.* 242, 118479 (2023).
30. B.K. Rai, C.A. Mizzi, A. Bretaña, L. Breton, C. Housley, D. Ivy, J. Abbott, B. Maiorov, B.R. Gautam, M. Frontzek, R.C. Rai, and S. Calder, Magnetic properties of $(Mo_{2/3}Dy_{1/3})_2AlC$ arc melted polycrystalline samples. *J. Magn. Magn. Mater.* 624, 172992 (2025).
31. M.S. Alam, M.A. Chowdhury, T. Khandaker, M.S. Hossain, M.S. Islam, M.M. Islam, and M.K. Hasan, Advancements in MAX phase materials: structure, properties, and novel applications. *RSC Adv.* 14, 26995 (2024).
32. J. Abbott, V. Morris, M. Adhikari, S. Balabhadra, A. Bretana, B. Rai, D. Autrey, and B. Gautam, Structural and morphological characteristics of rare earth element-based MAX Phase and MXene. *Microsc. Microanal.* 30(Suppl 1), 1215 (2024).
33. G. Kresse, and J. Hafner, *Ab initio* molecular dynamics for liquid metals. *Phys. Rev. B* 47, 558 (1993).
34. G. Kresse, and J. Furthmüller, Efficiency of ab-initio total energy calculations for metals and semiconductors using a plane-wave basis set. *Comput. Mater. Sci.* 6, 15 (1996).
35. J.P. Perdew, K. Burke, and M. Ernzerhof, Generalized gradient approximation made simple. *Phys. Rev. Lett.* 77, 3865 (1996).
36. W. Kohn, and L.J. Sham, Self-consistent equations including exchange and correlation effects. *Phys. Rev.* 140, A1133 (1965).
37. P.E. Blöchl, Projector augmented-wave method. *Phys. Rev. B* 50, 17953 (1994).
38. Q. Tao, J. Lu, M. Dahlqvist, A. Mockute, S. Calder, A. Petruhins, R. Meshkian, O. Rivin, D. Potashnikov, E.N. Caspi, H. Shaked, A. Hoser, C. Opagiste, R.M. Galera, R. Salikhov, U. Wiedwald, C. Ritter, A.R. Wildes, B. Johansson, L. Hultman, M. Farle, M.W. Barsoum, and J. Rosen, Atomically layered and ordered rare-earth i-MAX phases: a new class of magnetic quaternary compounds. *Chem. Mater.* 31, 2476 (2019).
39. M. Dahlqvist, J. Lu, R. Meshkian, Q. Tao, L. Hultman, and J. Rosen, Prediction and synthesis of a family of atomic laminate phases with Kagomé-like and in-plane chemical ordering. *Sci. Adv.* 3, e1700642 (2017).
40. A. Champagne, O. Chaix-Pluchery, T. Ouisse, D. Pinek, I. Gélard, L. Jouffret, M. Barbier, F. Wilhelm, Q. Tao, J. Lu, J. Rosen, M.W. Barsoum, and J.C. Charlier, First-order Raman scattering of rare-earth containing i -MAX single crystals $(Mo_{2/3}RE_{1/3})_2AlC$ (RE=Nd, Gd, Dy, Ho, Er). *Phys. Rev. Mater.* 3, 053609 (2019).
41. R. Sangavi, M. Keerthana, and T. Pushpa Malini, Design of an electrochemical sensor for the determination of riboflavin using cobalt doped dysprosium oxide nanocubes modified glassy carbon electrode. *Chem. Select* 7, e202201661 (2022).
42. S. Upadhyay, and O.P. Pandey, One-pot synthesis of pure phase molybdenum carbide (Mo_2C and MoC) nanoparticles for hydrogen evolution reaction. *Int. J. Hydrog. Energy* 45, 27114 (2020).
43. L. Nánai, R. Vajtai, and T.F. George, Laser-induced oxidation of metals: state of the art. *Thin Solid Films* 298, 160 (1997).